Iğdır Üniversitesi Fen Bilimleri Enstitüsü Dergisi, 15(3), 1008-1018, 2025
Journal of the Institute of Science and Technology, 15(3), 1008-1018, 2025

ISSN: 2146-0574, eISSN: 2536-4618

Kimya / *Chemistry* **DOI: 10.21597/jist.1561684**

Araştırma Makalesi / *Research Article*

Geliş tarihi / *Received*: 05.10.2024 **Kabul tarihi / *Accepted*: 11.04.2025**

Atıf İçin: Tanrıverdi, A. A. ve Yıldıko, Ü. (2025). 4-(2-(2-İzopropil-5-metilfenoksi) fenoksi) ftalonitril'in Alzheimer ve COVID-19 Enzimleriyle Moleküler Yerleştirme ve DFT Çalışmaları. *Iğdır Üniversitesi Fen Bilimleri Enstitüsü Dergisi*, 15(3), 1008-1018.

To Cite: Tanrıverdi, A. A. & Yıldıko, Ü. (2025). Molecular Docking of 4-(2-(2-Isopropyl-5-methylphenoxy) phenoxy) phthalonitrile with Alzheimer's and COVID-19 Enzymes and DFT Studies. *Journal of the Institute of Science and Technology*, 15(3), 1008-1018.

4-(2-(2-İzopropil-5-metilfenoksi) fenoksi) ftalonitril'in Alzheimer ve COVID-19 Enzimleriyle Moleküler Yerleştirme ve DFT Çalışmaları

Aslıhan Aycan TANRIVERDİ[1*], Ümit YILDIKO[2]

Öne Çıkanlar:
- 2-İzopropil-5-metilfenoksi
- Alzheimer ve COVID-19
- Yerleştirme puanı

Anahtar Kelimeler:
- Ftalonitril
- DFT hesaplamaları
- Moleküler yerleştirme

ÖZET:

Ftalonitriller, yüksek performanslı makromoleküllerin sentez ve formülasyonunda önemli bir bileşendir. Moleküler yapılar üzerine sistematik teorik çalışma, yeni terapötik bileşiklerin rasyonel bir şekilde yaratılması için esastır. Bu çalışma, yoğunluk fonksiyonel teorisi (DFT) ve moleküler yerleştirme üzerine sistematik teorik araştırma yürütmek için aromatik nitril tipi 4-(2-(2-İzopropil-5-metilfenoksi)fenoksi)ftalonitril (IMPN) kullanır. IMPN'nin geometri açısından optimize edilmiş yapıları, 6-311G(d,p) baz setiyle DFT/B3LYP ve B3PW91 yöntemleri kullanılarak incelenmiştir. MEP sonuçları, metilfenoksinin elektronik etkisinin siyano gruplarından elektronları çektiğini ve bunun da siyano karbonunu daha fazla açığa çıkardığını ve nükleofilik reaksiyona daha yatkın hale getirdiğini göstermektedir. Temsili farmakolojik olarak aktif bir kısım olan IMPN'nin moleküler yerleştirme analizi ve farmakolojik potansiyeli, asetilkolinesteraz (AChE) ve bütirilkolinesteraz (BChE) Alzheimer ve COVID-19 enzimlerine karşı inhibe edici kapasitesini belirlemek için değerlendirildi. Bir ligand olarak IMPN, enzim kristal yapılarıyla -8.243, -7.920 ve -7.368 kcal/mol'lük etkili yerleştirme puanları gösterdi.

Molecular docking of 4-(2-(2-Isopropyl-5-methylphenoxy) phenoxy) phthalonitrile with Alzheimer's and COVID-19 enzymes and DFT studies

Highlights:
- 2-Isopropyl-5-methylphenoxy
- Alzheimer's and COVID-19
- Docking Score

Keywords:
- Phthalonytrile
- DFT calculations
- Molecular docking

ABSTRACT:

Phthalonitriles are a crucial component in the synthesis and formulation of high-performance macromolecules. Systematic theoretical study on molecular structures is essential for the rational creation of novel therapeutic compounds. This study takes aromatic nitrile type 4-(2-(2-Isopropyl-5-methylphenoxy)phenoxy)phthalonitrile (IMPN) to conduct systematic theoretical research on density functional theory (DFT) and molecular docking. The geometry-optimized structures of IMPN were examined using the DFT/B3LYP and B3PW91 methods with the 6-311G(d,p) basis set. The MEP results show that the electronic effect of methylphenoxy attracts electrons from cyano groups, which makes the cyano carbon more exposed and more prone to nucleophilic reaction. The molecular docking analysis and pharmacological potential of IMPN, as a representative pharmacologically active moiety, were assessed to ascertain its inhibitory capacity against acetylcholinesterase (AChE), and butyrylcholinesterase (BChE) Alzheimer's and COVID-19 enzymes. IMPN, as a ligand, demonstrated effective docking scores of -8.243, -7.920, and -7.368 kcal/mol with the enzyme crystal structures.

[1*]Aslıhan Aycan TANRIVERDİ (**Orcid ID:** 0000-0001-5811-8253), Kafkas Üniversitesi, Fen Edebiyat Fakültesi, Kimya Bölümü, Kars, Türkiye
[2]Ümit YILDIKO (**Orcid ID:** 0000-0001-8627-9038), Kafkas Üniversitesi, Mühendislik ve Mimarlık Fakültesi, Biyomühendislik, Kars, Türkiye

***Sorumlu Yazar/*Corresponding Author**: Aslıhan Aycan TANRIVERDİ, e-mail: t.aslihanaycan@gmail.com

INTRODUCTION

Phthalonitrile is an aromatic cyano crosslinking monomer widely used in materials science. Through a nucleophilic crosslinking mechanism, cyano groups contribute to the formation of thermally stable compounds such as phthalocyanine, isoindoline, and triazine, making it suitable for molecular design applications. Functional cyano structures on phthalonitrile are generally chemically inert, requiring higher temperatures for cross-linking reactions (Gao et al.,2023). This problem causes high processing energy consumption of the material and results in processing temperatures that are incompatible with other materials (Gao et al., 2024). Therefore, composite modification and large-scale applications are limited. Since the internal chemical structural environments significantly affect the reactivity of cyano groups, new designs based on molecular engineering will be effective in increasing the binding capacity of aromatic nitriles (Yang et al., 2024). Quantum mechanics, which is especially useful for characterizing the dimensional structure of molecules using their electronic structure and characteristics, provides the basis for the study of electrons in quantum chemistry (Han et al., 2014; Kolesnikova et al., 2022). It is capable of measuring molecules' dimensional architecture with accuracy. Because of this, quantum chemistry plays a significant role in molecular engineering and is frequently used to calculate intermolecular interactions and simulate reaction pathways, among other things, to disclose features of molecules (Giricheva et al., 2015). Phthalonitrile-related quantum chemistry research can aid in our comprehension of the mechanisms underlying the cyano alterations in the phenol ring and how they affect the chemical environment (Tunç et al., 2021; He et al., 2023). This could encourage its more strategic application in materials science and enhance the ideas behind molecular design to create materials with superior functionality such as phthalocyanines (Cabir et al., 2020; Ağırtaş et al., 2021).

This study with DFT methods to study optimazition of IPMN compound compared the research results in the literature and its pharmacological properties were investigated. With DFT calculations ve molecular docking, we have gained more information about the bonding properties, charge distributions and electron delocalization of IPMN compound and studied the intermolecular interactions between the two methods. We investigated the bonding properties, charge distributions and electron delocalization of IPMN compound with DFT calculations and molecular docking and the agreement between the two methods. This research method shows some physical, chemical and biological properties of IPMN compound.

MATERIALS AND METHODS

The dipole moment is indeed a key property (Frisch et al., 2016; Priya et al., 2019). The DFT/B3LYP and B3PW91 methods with the 6-311G(d,p) basis set were chosen due to their proven accuracy in predicting molecular geometry, electronic structure, and reactivity of organic compounds. The B3LYP functional is widely used for its balance between computational efficiency and precision, while B3PW91 provides an alternative approach to electron correlation effects. The 6-311G(d,p) basis set enhances the reliability of calculations by incorporating polarization functions, making it suitable for studying the electronic properties of IMPN. The ground state optimized structure was utilized to determine various parameters such as MEP and HOMO-LUMO. GaussView 06 software was utilized in order to obtain orbital energy spectra of frontiers.

RESULTS AND DISCUSSION

Geometry Optimization

Figure 1 displays the IPMN optimized gas phase structure, total Mulliken atomic charge, and bond lengths. Optimized bond lengths are computed using the DFT techniques. It was done to compare two IPMN compound optimization techniques. This indicates that the structure's potential energy is at its lowest. In the phenyl rings, every bond length and bond angle falls within the typical range. The phenyl rings at C-C bond lengths of 1.399-1.548Å for B3LYP, 1.393-1.549 Å for B3PW91, and 1.404Å for these values for C-O. The C-H bond lengths in the aromatic ring range from 1.081 to 1.092 Å, while the C-N bond length falls between 1.165 and 1.167 Å. All C-C-C angles are between 110° and 120°, and the C-C-H angles in the compound range from 110° to 119°. The C-C-O angles are between 121° and 123°, and the C-C-N angles are approximately 178.10° to 178.15°, as calculated using the B3LYP and B3PW91 methods, respectively. While both methods often yield similar results, especially for well-behaved systems, there can be subtle differences in accuracy, particularly for specific properties or systems. The differences in the underlying functionals can lead to variations in predicted geometries, energies, and properties like vibrational frequencies or reaction barriers.

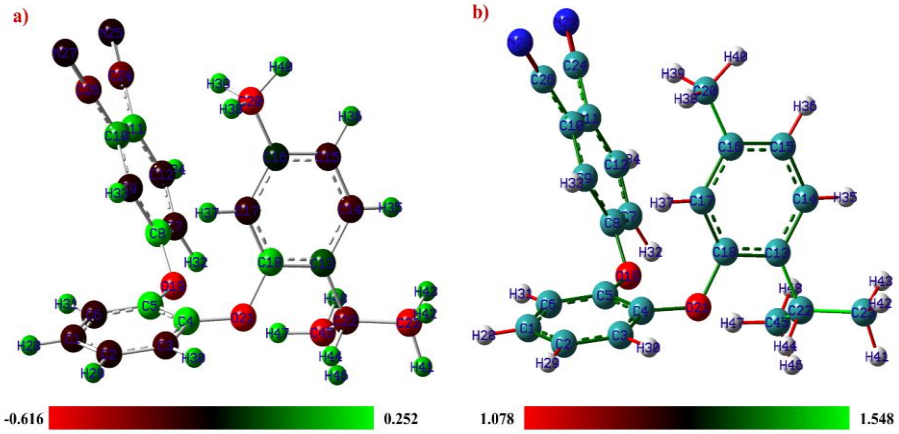

Figure 1. Optimized structures of the DBP compound from a different perspective a) Mulliken atomic charge b) bond lenghts

The dipole moment is crucial for understanding molecular interactions with electric fields. It can be estimated by calculating the total distribution of positive and negative charges. Table 1 presents the calculated datas, including the electronic dipole moment parameters. The dipole moment ranges from 6.114 to 6.121 D, indicating that the title molecule exhibits characteristics of a nonlinear optical material.

Table 1. Electric dipole moments (in Debye), polarizabilities (in atomic units), β components (esu) of IPMN values were calculated with the DFT methods

Parameters	DFT/B3LYP	DFT/B3PW91	Parameters	DFT/B3LYP	DFT/B3PW91
μ_x	-5.167	-5.195	β_{XXX}	-344.934	--356.819
μ_y	2.695	2.649	β_{XXY}	78.888	80.155
μ_z	-1.849	-1.859	β_{XYY}	-51.530	-53.035
μ (D)	**6.114**	**6.121**	β_{YYY}	74.289	74.306
α_{xx}	-211.441	-210.231	β_{XXZ}	-53.478	-56.039
α_{yy}	-150.824	-149.539	β_{XYZ}	-24.927	-23.7962
α_{zz}	-163.552	-161.956	β_{YYZ}	16.657	18,925
α_{XY}	9.649	10,666	β_{XZZ}	-20.154	-23.841
α_{XZ}	-16.256	-12.669	β_{YZZ}	-20.811	-22.553
α_{YZ}	2.295	2.677	β_{ZZZ}	-28.840	-28.757
α (au)	**-175.273**	**-174.964**	**β (esu)**	**$1.96x10^{-28}$**	**$1.95x10^{-28}$**

Molecular Orbitals: HOMO - LUMO

The Highest Occupied Molecular Orbital (HOMO) and Lowest Unoccupied Molecular Orbital (LUMO) are critical in understanding the behavior of electrons in a molecule (Mumit et al., 2020; Sherin et al., 2020; Shukla and Yadava, 2022). The energy difference between the HOMO and LUMO orbitals is crucial for determining the reactivity of a molecule. A smaller gap typically indicates that the molecule is more reactive, as electrons can more easily transition between these two orbitals. Conversely, a larger gap suggests a more stable molecule with lower reactivity. The EHOMO and ELUMO values calculated DFT methods were -6.912 eV and -6.422 eV, respectively, as shown in Figure 2a. The bandgap values calculated using both methods are close to each other. The HOMO-LUMO energy gap, ranging between 4.463 and 3.918 eV, suggests that the molecule is softer, more reactive, and highly polarizable (Maidur et al., 2017). The HOMO-LUMO energy gap, which ranges from 4.463 to 3.918 eV, indicates the molecule is more reactive, chemical softer, and highly polarizable.

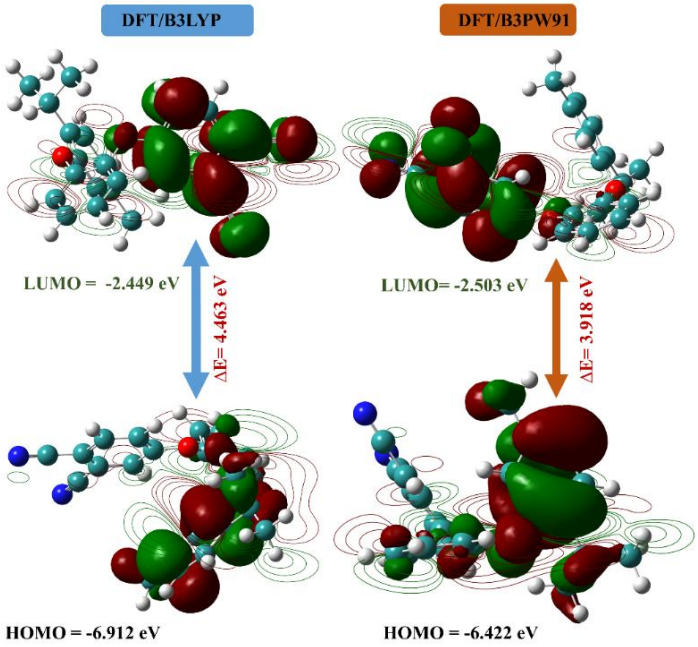

Figure 2. Frontier orbitals energy composition of the molecule

Table 2. Molecular Energy descriptors of IPMN

Molecular Energy	**DFT/B3LYP**	**DFT/B3PW91**
E_{LUMO}	-2.449	-2.503
E_{HOMO}	-6.912	-6.422
Energy deficit (Δ)E_{HOMO} -E_{LUMO}	4.463	3.918
Ionization Potential ($I=-E_{HOMO}$)	6.912	6.422
Electron Relevance ($A=-E_{LUMO}$)	2.449	2.503
Global Hardness ($\eta=(I-A)/2$)	2.231	1.959
Global Softness ($s=1/2\eta$)	0.224	0.255
Chemical potential ($\mu=(I+A)/2$)	4.680	4.463
Electronegativity ($\chi=(1+A)/2$)	1.724	1.752
Global Electrophilicity ($\omega=\mu^2/2\eta$)	4.910	5.080

Molecular electrostatic potential (MEP)

MEP maps are generated to assess the amount and distribution of the electrostatic potential of the molecular structure (Moghadam et al., 2019). MEP maps provide crucial information about a molecule's reactivity, interactions, and binding behavior. They are particularly valuable in fields like biochemistry and drug design, where understanding interactions with target molecules is essential. The MEP reactive sites were calculated using DFT/B3LYP and B3PW91 methods with the 6-311G (d,p) basis set, as depicted in Figure 3. The various colors in the molecule represent different electrostatic potentials, with potential levels shifting to more negative regions as follows: blue > green > yellow > orange > red. The values for the negative potential (red regions) V(r) are -5.666 e-2, while the predominant positive potentials (blue regions) are approximately 5.666 e-2 for phthalonitrile. These calculations take into account atomic-level charge distributions and molecular geometries (Cabir et al., 2019; Cabir et al., 2020; Ağırtaş et al., 2021). Together, the analysis of active sites and MEP provides a comprehensive understanding of the chemical and biological activities of a compound. By integrating structural, electrostatic, and interaction data, researchers can better predict the behavior of compounds in chemical reactions and biological systems, ultimately guiding the design of more effective therapeutic agents.

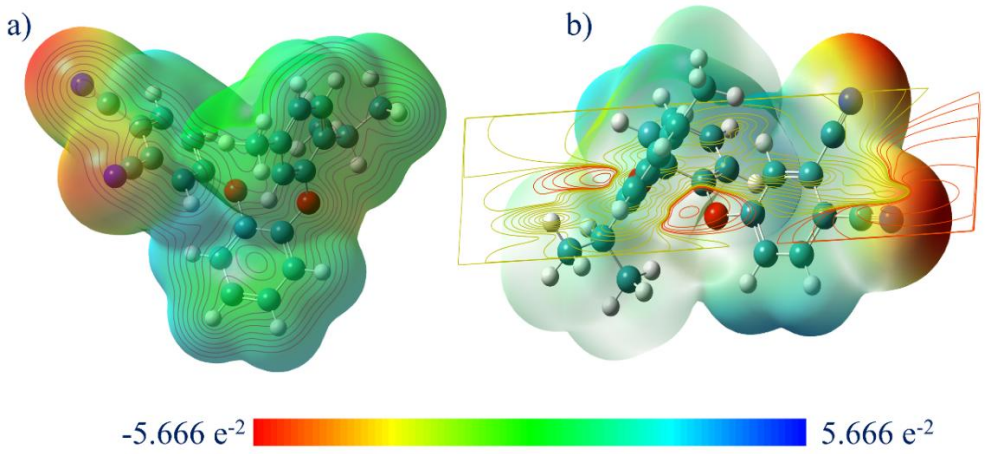

Figure 3. MEP reactive sites of IPMN with (a) B3LYP and (b) B3PW91

Molecular docking studies

In the drug design study, the he selection of the 7RN4-coded protein is crucial as it provides a high-resolution structure of the SARS-CoV-2 main protease (M pro), which is essential for accurately studying inhibitor interactions and optimizing drug design. The selection of the 6QAE-coded protein is important as it provides a detailed structural representation of human butyrylcholinesterase (BChE), which is crucial for understanding the binding interactions of tryptophan-based inhibitors and optimizing their therapeutic potential against Alzheimer's disease. The selection of the 5HF9-coded protein is significant as it provides crucial structural insights into human acetylcholinesterase inhibited by organophosphates and bound to oximes, aiding the design of more effective reactivators for treating organophosphate poisoning. This protein structures were obtained from the RCSB (http//www.rcsb.org/pdb) (Considering those with RMSD values less than 2.4 Å, there is no mutation.) Docking of a precursor fragment of the ligand of IPMN into some protein receptors were made using the Maestro (ver. 11.8) software's Protein Prep., Grid Gen, and Lig Prep modules. Docking analyses were conducted based on the literature regarding ligand-protein interactions (Kalaimathi et al., 2021; Alshehri et al., 2022; Fatriansyah et al., 2022; Keşkek Karabulut et al., 2024). Molecular docking

analyses were performed using the Glide docking subprogram in the Maestro program. In silico working images were presented with Discovery Studio 2017 (Biovia, 2017) and Maestro.

Drug potential of the phthalonitrile

Pharmacokinetic analysis

Pharmacokinetics refers to the study of how a drug is absorbed, distributed, metabolized, and excreted (ADME) in the body. Understanding these properties is essential for predicting the drug's behavior within a biological system. Assessing the pharmacokinetic properties and conducting ADMET profiling are crucial steps in the drug development process, particularly for molecules designed as enzyme inhibitors. These evaluations help ensure that drug candidates are safe, effective, and suitable for further development. Understanding these properties can significantly improve the chances of successful clinical translation and therapeutic application (Table 3) (Chagas et al., 2018; Athar Abbasi et al., 2019; Sudhapriya at al., 2019). Rotatable bonds within the active groups of a drug candidate molecule increase flexibility, allowing better adaptation to the binding site. The evaluated moiety contains five rotatable bonds, providing sufficient flexibility (Alswaidan et al., 2017; Elangovan et al., 2022). The Log P value, which serves as an indicator of molecular hydrophobicity or lipophilicity, was approximately 5. This value is considered favorable for achieving optimal cell membrane permeability. The “colour region” in Figure 4 represents the physicochemical range where oral bioavailability is sufficient (Alswaidan et al., 2017; Sudhapriya at al., 2019; Chtita et al., 2019; Elangovan et al., 2022).

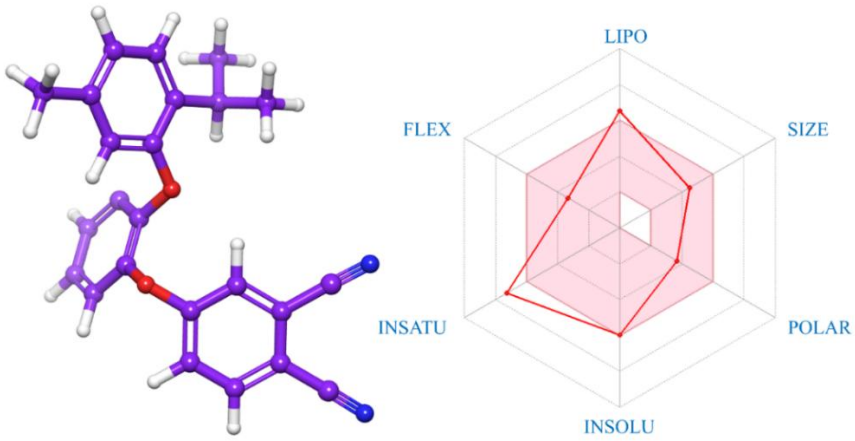

Figure 4. MEP reactive sites of IPMN with (a) B3LYP and (b) B3PW91

Table 3. Potential analysis of drug candidate compound IPMN

Compound IPMN	Physicochemical properties								
Lip.cons. log P	TPSA[a] (A^2)	MR[b]	% ABS[c]	H-bond don.	H-bond acc.	Rot. bond	Aromatic heavy atoms	Heavy atoms	MW[d] g/mol
5.11	66.04	108.45	86.09	0	4	5	18	28	368.43

[a]**TPSA**, topological polarsurface area; [b]**MR**, molar refractivity; [d]**%ABS:**percentage of absorption (%ABS= 109−[0.345×TPSA]; [d]**MW**, molecular weight;

In-silico studies

Molecular docking is useful for determining the performance as an enzyme inhibitor using binding poses in the AChE and BChE proteins involved of a drug candidate in Alzheimer's disease (Cheng et al., 2019; Larik et al., 2020; Aras et al., 2021) and flexible SARS-CoV-2 proteins (Alghamdi et al., 2021; Hall-Swan et al., 2021). In addition, a good docking score was obtained by performing an in silico study,

in which the effect of the covid protein was determined theoretically. To simulate these COVID 19 and Alzheimer's disease treatments, the binding modes of IPMN to its receptors and their numerical data are presented in Table 4.

Table 4. Compound 3-protein binding affinity scores (kcal/mol)

Compound IPMN	Docking Score (kcal/mol)		
	AChE (PDB: 5HF9)	BChE (PDB:6QAE)	SARS-CoV-2 (PDB: 7RN4)
3	-8.243	-7.920	- 7.368

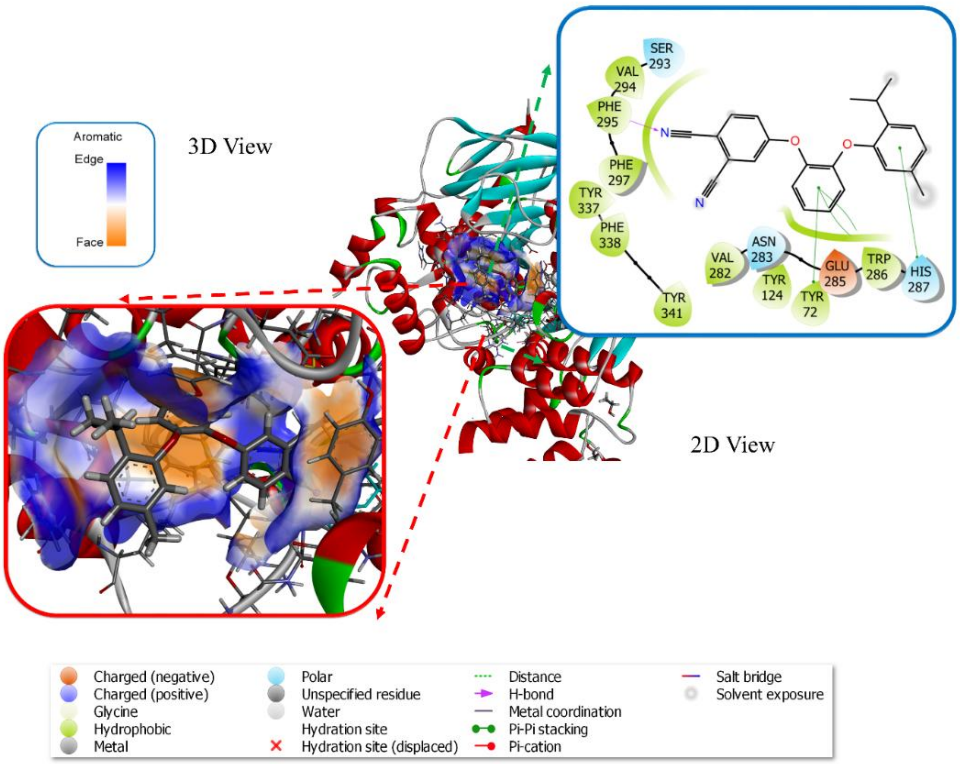

Figure 5. 3D View and 2D View the interaction mode between the phthalonitrile (**3)** - AChE

Acetylcholinesterase (AChE) proteins are commonly targeted to alleviate the effects of dementia associated with AD (Franklin et al., 2016; Adiguzel et al., 2021; Yildiko et al., 2021). The phthalonitrile IPMN showed a good binding performance of 8.243 kcal/mol and it is a strong AChE inhibitor. It bonds with HIS 287 (6.13 Å) TYR 72 (5.69 -5.77 Å), TRP 286 (5.69 Å) π-alkyl, PHE 295 (4.76 Å), conventional Hydrogen Bond, VAL 294 (4.20) carbon-hydrogen bond VAL 282, ASN 283, TYR 337, TYR 124 van der Waals, TYR 72 (3.94 Å), TRP The 286 is (3.74 Å), π -π stacked and (5.31 Å) π T-shaped, and the TYR 341 (5.54 Å), π-π stacked. The binding of the IPMN and AChE protein via the aromatic surface at the best pose was mapped and shown in Figure 5.

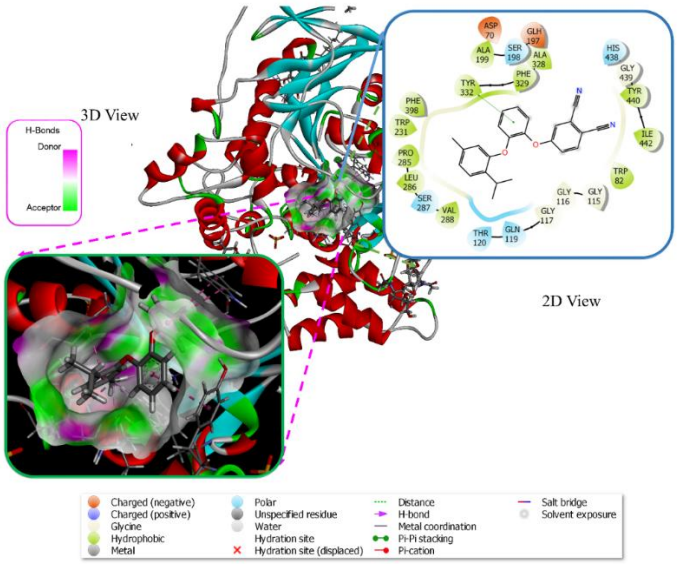

Figure 6. 3D View and 2D View the interaction mode of the phthalonitrile - BChE enzyme

In studies against Alzheimer's disease, there are many crystal structures as a Tryptophan-based selective nanomolar butyrylcholinesterase (BChE) protein (Meden et al., 2019; Yildiko et al., 2021). A docking study showing the new binding mode of the synthesized phthalonitrile compound with human BChE was performed and a docking score of -7.920 kcal/mol was calculated. The binding performance is a very successful result for in silico inhibition of the compound (Atalar et al., 2021). It can be considered as a ligand for symptomatic treatment against Alzheimer's disease. Protein-ligand interaction TRP 82 (5.11 Å) π-π stacked, TYR 332 π-π T- shaped, GLY 116 Amide - π stacked, GLY 439 (3.89 Å) carbon-hydrogen bond, PHE 398 (6.19 Å), TRP 231 (4.86 Å), PHE 329 (6.67 Å) π-alkyl, VAL 288, GLY 117, ALA 199, PRO285 GLY, and SER 198 van der Waals bonds were calculated by ligand docking. Phthalonitrile working as an inhibitor and binding to the BChE backbone is mapped to the hydrogen bonds protein surface and is shown in Figure 6.

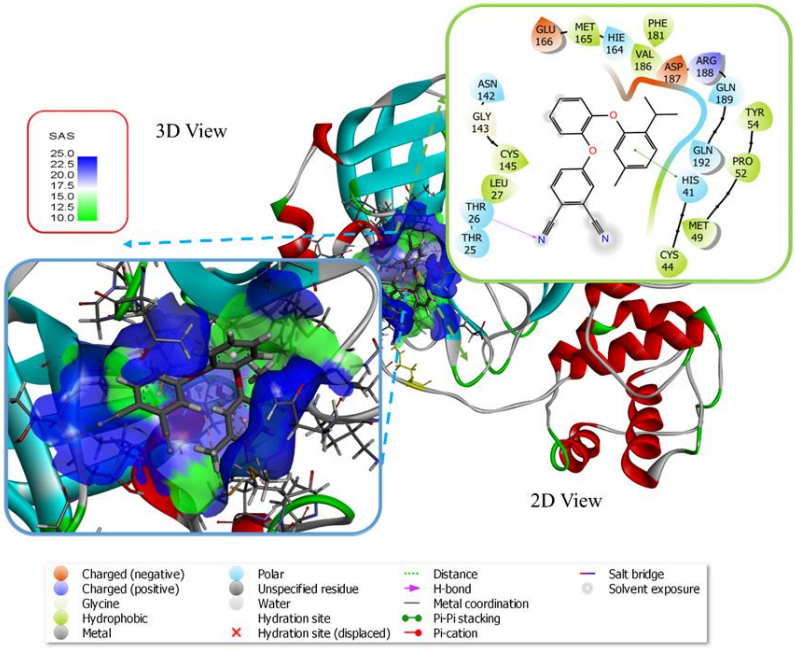

Figure 7. 3D View and 2D View the interaction mode of the phthalonitrile - SARS-CoV-2 protein

Synthesizing small molecule antivirals suitable for Coronavirus 2 (SARS-CoV-2) proteins, which are effective all over the world and show severe acute respiratory syndrome, is very important in fighting this disease COVID-19 (Rudrapal et al., 2022). SARS-CoV-2, which is effective in ligand binding, is a drug protein used to determine the performance of enzyme inhibitors (Kneller et al., 2021). IPMN interacted with the SARS-CoV-2 protease docking score, a good value of -7,368 kcal/mol. These interactions are respectively; Ligand-protein interaction, THR 26 (2.41 Å) conventional hydrogen bond, CYS 145 (4.94 Å), HIS 41 (4.11 Å) π-π stacked, HIS 41 2.63 carbon-hydro (5.37 Å) π- alkyl, MET 165 (3.79-3.95 Å), MET 49 (4.02- 4.99 Å), CYS 44 (4.43-2.43 Å) alkyl and VAL 186, GLN 189, THR 25, ASN 142, ARG 188 van der Waals bondings were performed. Figure 7 shows it flexibly attached to the protein's catalytic site.

CONCLUSION

Quantum chemical computations have been used to perform in-depth studies on the IPMN molecule. The electronic, and structural of the molecule were computed with the DFT / B3LYP and B3PW91 techniques. The structural parameters were calculated theoretically. It was determined that the IPMN under investigation may function as a nonlinear optical (NLO) material. Furthermore, Mulliken charges, HOMO-LUMO maps, and MESP were seen, suggesting that it is a good intermediate material for syntheses. Future synthesis studies can benefit greatly from taking this data into account as it can reduce chemical consumption and facilitate crucial predictions during the synthesis of compounds. Molecular docking revealed that IPMN has a higher affinity and stronger binding energy against AChE and BChE compared to standard treatments for Alzheimer's. The in-silico studies produced results suggesting that this molecule should be considered in drug design processes for therapeutic applications. All things considered, this work demonstrates the remarkable pharmacological properties of IPMN as a potential bioactive substance.

Conflict of Interest

The article authors declare that there is no conflict of interest between them.

Author’s Contributions

The authors declare that they have contributed equally to the article.

REFERENCES

Adiguzel, R., et al. (2021). Synthesis and in silico studies of Novel Ru(II) complexes of Schiff base derivatives of 3-[(4-amino-5-thioxo-1,2,4-triazole-3-yl)methyl]-2(3H)-benzoxazolone compounds as potent Glutathione S-transferase and Cholinesterases Inhibitor. *Journal of Molecular Structure*, 1231, 129943.

Ağırtaş, M.S., et al. (2021). Synthesis, antioxidant, DNA cleavage and antimicrobial properties of phthalocyanine complexes bearing the poly-hydroxyl groups. *Chemical Papers*, 75(4), 1749-1760.

Alghamdi, H.A., et al. (2021). Repurposing the inhibitors of COVID-19 key proteins through molecular docking approach. *Process Biochemistry*, 110, 216-222.

Alshehri, B., et al. (2022). Molecular target prediction and docking of anti-thrombosis compounds and its activation on tissue-plasminogen activator to treat stroke. *Journal of King Saud University - Science*, 34(1), 101732.

Alswaidan, I.A., et al. (2017). 2,4-Ditellurouracil and its 5-fluoro derivative: Theoretical investigations of structural, energetics and ADME parameters. *Computational Biology and Chemistry*, 68, 56-63.

Aras, A., et al. (2021). Biochemical constituent, enzyme inhibitory activity, and molecular docking analysis of an endemic plant species, Thymus migricus. *Chemical Papers*, 75(3), 1133-1146.

Atalar, M.N., et al. (2021). The effects of Daucus carota extract against PC3, PNT1a prostate cells, acetylcholinesterase, glutathione S-transferase, and α-glycosidase; an in vitro–in silico study. *Journal of Food Biochemistry*, 45(12), e13975.

Athar Abbasi, M., et al. (2019). Synthesis of novel N-(1,3-thiazol-2-yl)benzamide clubbed oxadiazole scaffolds: Urease inhibition, Lipinski rule and molecular docking analyses. *Bioorganic Chemistry*, 83, 63-75.

Biovia, D.S., (2017). Discovery studio modeling environment. Release.

Cabir, B., et al. (2020). Computational DFT calculations, photovoltaic properties and synthesis of (2R, 3S)-2, 3, 4-trihydroxybutoxy substituted phthalocyanines. *Inorganic and Nano-Metal Chemistry*, 50(9), 816-827.

Cabir, B., Yildiko, U. and Ağirtaş, M. S. (2019). Synthesis, DFT analysis, and electronic properties of new phthalocyanines bearing ETAEO substituents on peripheral position. *Journal of Coordination Chemistry*, 72(17), 2997-3011.

Chagas, C. M., Moss, S. and Alisaraie, L. (2018). Drug metabolites and their effects on the development of adverse reactions: Revisiting Lipinski's Rule of Five. *International Journal of Pharmaceutics*, 549(1), 133-149.

Cheng, Z.-Q., et al. (2019). Molecular-docking-guided design and synthesis of new IAA-tacrine hybrids as multifunctional AChE/BChE inhibitors. *Bioorganic Chemistry*, 83, 277-288.

Chtita, S., et al. (2019). QSAR study of anti-Human African Trypanosomiasis activity for 2-phenylimidazopyridines derivatives using DFT and Lipinski's descriptors. *Heliyon*, 5(3), e01304.

Elangovan, N., Thomas, R. and Sowrirajan, S. (2022). Synthesis of Schiff base (E)-4-((2-hydroxy-3,5-diiodobenzylidene)amino)-N-thiazole-2-yl)benzenesulfonamide with antimicrobial potential, structural features, experimental biological screening and quantum mechanical studies. *Journal of Molecular Structure*, 1250, 131762.

Fatriansyah, J. F., et al. (2022). Molecular docking and dynamics studies on propolis sulabiroin-A as a potential inhibitor of SARS-CoV-2. *Journal of King Saud University-Science*, 34(1), 101707.

Franklin, M. C., et al. (2016). Structures of paraoxon-inhibited human acetylcholinesterase reveal perturbations of the acyl loop and the dimer interface. *Proteins*, 84(9), 1246-56.

Frisch, M. J., et al. (2016). GAUSSIAN 09. http://www.gaussian.com/.

Gao, M., et al. (2023). Novel liquid phthalonitrile monomers towards high performance resin. *European Polymer Journal*, 191, 112027.

Gao, M., et al. (2024). Rediscovering phthalonitrile resins: a novel liquid monomer towards high-performance resins††Electronic supplementary information (ESI) available. See DOI: https://doi.org/10.1039/d4py00100a. *Polymer Chemistry*, 15(21), 2157-2166.

Giricheva, N. I., et al. (2015). The difference between gas-phase and crystal structures of ortho-nitromethylbenzenesulfonate. Conformation variety study of free molecules by electron diffraction and quantum chemistry. *Journal of Molecular Structure*, 1085, 191-197.

Hall-Swan, S., et al. (2021). DINC-COVID: A webserver for ensemble docking with flexible SARS-CoV-2 proteins. *Computers in Biology and Medicine*, 139, 104943.

Han, K., et al. (2014). Quantum chemistry study on nonlinear optical properties of hemicyanine dye derivatives with different electron donor groups. *Computational and Theoretical Chemistry*, 1044, 24-28.

He, X., et al. (2023). A theoretical investigation on the chemical environment of pyrazine-2,3-dicarbonitrile and phthalonitrile: Density functional theory (DFT) calculation and experimental verification. *Journal of Molecular Structure*, 1292, 136117.

Kalaimathi, K., et al. (2021). Molecular docking and network pharmacology-based approaches to explore the potential of terpenoids for Mycobacterium tuberculosis. *Pharmacological Research - Modern Chinese Medicine*, 1, 100002.

Keşkek Karabulut, Y., et al. (2024). MAO-A Inhibitor Properties by Molecular Modeling Method, Antimicrobial Activity and Characterization of Silver Nanoparticles Synthesized from Lactifluus Bertillonii Mushroom. *Düzce Üniversitesi Bilim ve Teknoloji Dergisi*, 4, 2033-2049.

Kneller, D. W., et al. (2021). Structural, Electronic, and Electrostatic Determinants for Inhibitor Binding to Subsites S1 and S2 in SARS-CoV-2 Main Protease. *Journal of medicinal chemistry*, 64(23), 17366-17383.

Kolesnikova, I. N., et al. (2022). Equilibrium molecular structure of nicotinic acid hydrazide: joint study by means of gas electron diffraction and quantum chemistry. *Journal of Molecular Structure*, 1253, 132281.

Larik, F. A., et al. (2020). Synthesis, inhibition studies against AChE and BChE, drug-like profiling, kinetic analysis and molecular docking studies of N-(4-phenyl-3-aroyl-2(3H)-ylidene) substituted acetamides. *Journal of Molecular Structure*, 1203, 127459.

Maidur, S. R., et al. (2017). Experimental and computational studies on second-and third-order nonlinear optical properties of a novel D-π-A type chalcone derivative: 3-(4-methoxyphenyl)-1-(4-nitrophenyl) prop-2-en-1-one. *Optics & Laser Technology*, 97, 219-228.

Meden, A., et al. (2019). Tryptophan-derived butyrylcholinesterase inhibitors as promising leads against Alzheimer's disease. *Chemical communications (Cambridge, England)*, 55(26), 3765-3768.

Mumit, M. A., et al. (2020). DFT studies on vibrational and electronic spectra, HOMO–LUMO, MEP, HOMA, NBO and molecular docking analysis of benzyl-3-N-(2,4,5-trimethoxyphenylmethylene)hydrazinecarbodithioate. *Journal of Molecular Structure*, 1220, 128715.

Priya, M. K., et al. (2019). Molecular Structure, Spectroscopic (FT-IR, FT-Raman, 13C and 1H NMR) Analysis, HOMO-LUMO Energies, Mulliken, MEP and Thermal Properties of New Chalcone Derivative by DFT Calculation. *Materials Today: Proceedings*, 8, 37-46.

Rudrapal, M., et al. (2022). Repurposing of phytomedicine-derived bioactive compounds with promising anti-SARS-CoV-2 potential: Molecular docking, MD simulation and drug-likeness/ADMET studies. *Saudi Journal of Biological Sciences*, 29(4), 2432-2446.

Sherin, D. R. and Manojkumar, T. K. (2020). Significance of five membered heterocycles in fine tuning of HOMO-LUMO gap of simple donor-acceptor system as organic solar cell material: A DFT approach. *Materials Today: Proceedings*, 33, 1229-1233.

Shukla, B. K. and Yadava U. (2022). DFT calculations on molecular structure, MEP and HOMO-LUMO study of 3-phenyl-1-(methyl-sulfonyl)-1H-pyrazolo[3,4-d]pyrimidine-4-amine. *Materials Today: Proceedings*, 49(8), 3056-3060.

Sudhapriya, N., et al. (2019). Cu-mediated synthesis of differentially substituted diazepines as AChE inhibitors; validation through molecular docking and Lipinski's filter to develop novel anti-neurodegenerative drugs. Bioorganic & Medicinal Chemistry Letters, 29(11), 1308-1312.

Wang, D., et al., (2024). Enhanced mechanical and thermal properties of phenolic-type phthalonitrile nanocomposites with fumed silica nanoparticles. *Polymer*, 296, 126783.

Yang, W., et al. (2024). Aromatic nitrile resins with improved processability and thermal properties prepared by collaborative design of structure and blending strategy. *European Polymer Journal*, 216, 113247.

Yildiko, Ü., et al. (2021). Synthesis, enzymes inhibitory properties and characterization of 2- (bis (4-aminophenyl) methyl) butan-1-ol compound: Quantum simulations, and in-silico molecular docking studies. *Journal of the Indian Chemical Society*, 98(11), 100206.